Supplement of Biogeosciences, 15, 5031–5045, 2018
https://doi.org/10.5194/bg-15-5031-2018-supplement

Biogeosciences
Open Access

Supplement of

Diffusion limitations and Michaelis–Menten kinetics as drivers of combined temperature and moisture effects on carbon fluxes of mineral soils

Fernando Esteban Moyano et al.

Correspondence to: Fernando Esteban Moyano (fmoyano@uni-goettingen.de)

Model M2-dif steady state equations

The equilibrium solutions to the C pools of model M2-dif are given by:

$$C_P = K_D r_{ed} z(-2gI_{ml} f_{ge} f_{ug} r_{md} + 2gI_m f_{ug} r_{md} - 2gI_{sl} f_{ge} r_{mr} f_{ug} - 2gI_{sl} f_{ge} f_{ug} r_{md} + 2gI_{sl} r_{mr} + 2gI_{sl} r_{md} - I_{ml} f_{ge} f_{ug} r_{ed} r_{md} + I_{ml} f_{ug} r_{ed} r_{md} - I_{sl} f_{ge} r_{mr} f_{ug} r_{ed} - I_{sl} f_{ge} f_{ug} r_{ed} r_{md} + I_{sl} r_{mr} r_{ed} + I_{sl} r_{ed} r_{md})/(gI_{ml} V_D f_{ge} r_{mr} f_{ug} + gI_{ml} V_D f_{ge} f_{ug} r_{md} + 2gI_{ml} f_{ge} f_{ug} r_{ed} r_{md} - 2gI_{ml} f_{ug} r_{ed} r_{md} + gI_{sl} V_D f_{ge} r_{mr} f_{ug} + gI_{sl} V_D f_{ge} f_{ug} r_{md} + 2gI_{sl} f_{ge} r_{mr} f_{ug} r_{ed} + 2gI_{sl} f_{ge} f_{ug} r_{ed} r_{md} - 2gI_{sl} r_{mr} r_{ed} - 2gI_{sl} r_{ed} r_{md} + I_{ml} f_{ge} f_{ug} r_{ed}^2 r_{md} - I_{ml} f_{ug} r_{ed}^2 r_{md} + I_{sl} f_{ge} r_{mr} f_{ug} r_{ed}^2 + I_{sl} f_{ge} f_{ug} r_{ed}^2 r_{md} - I_{sl} r_{mr} r_{ed}^2 - I_{sl} r_{ed}^2 r_{md}) \tag{S1}$$

$$C_D = -z(r_{mr} + r_{md})/(gV_U f_{ug}(f_{ge} - 1)) \tag{S2}$$

$$C_M = f_{ug}(I_{ml} f_{ge} - I_{ml} + I_{sl} f_{ge} - I_{sl})/(f_{ge} r_{mr} f_{ug} - r_{mr} + f_{ug} r_{md} - r_{md}) \tag{S3}$$

$$C_{ED} = -g f_{ge} f_{ug}(I_{ml} r_{mr} + I_{ml} r_{md} + I_{sl} r_{mr} + I_{sl} r_{md})/(r_{ed}(2g f_{ge} r_{mr} f_{ug} - 2g r_{mr} + 2g f_{ug} r_{md} - 2g r_{md} + f_{ge} r_{mr} f_{ug} r_{ed} - r_{mr} r_{ed} + f_{ug} r_{ed} r_{md} - r_{ed} r_{md})) \tag{S4}$$

$$C_{EM} = -f_{ge} f_{ug}(gI_{ml} r_{mr} + gI_{ml} r_{md} + gI_{sl} r_{mr} + gI_{sl} r_{md} + I_{ml} r_{mr} r_{ed} + I_{ml} r_{ed} r_{md} + I_{sl} r_{mr} r_{ed} + I_{sl} r_{ed} r_{md})/(r_{ed}(2g f_{ge} r_{mr} f_{ug} - 2g r_{mr} + 2g f_{ug} r_{md} - 2g r_{md} + f_{ge} r_{mr} f_{ug} r_{ed} - r_{mr} r_{ed} + f_{ug} r_{ed} r_{md} - r_{ed} r_{md})) \tag{S5}$$

In these equations, I_{ml} and I_{sl} are metabolic and structural litter input, which represent litter additions to the C_D and C_P pools, respectively.

Supplementary figures

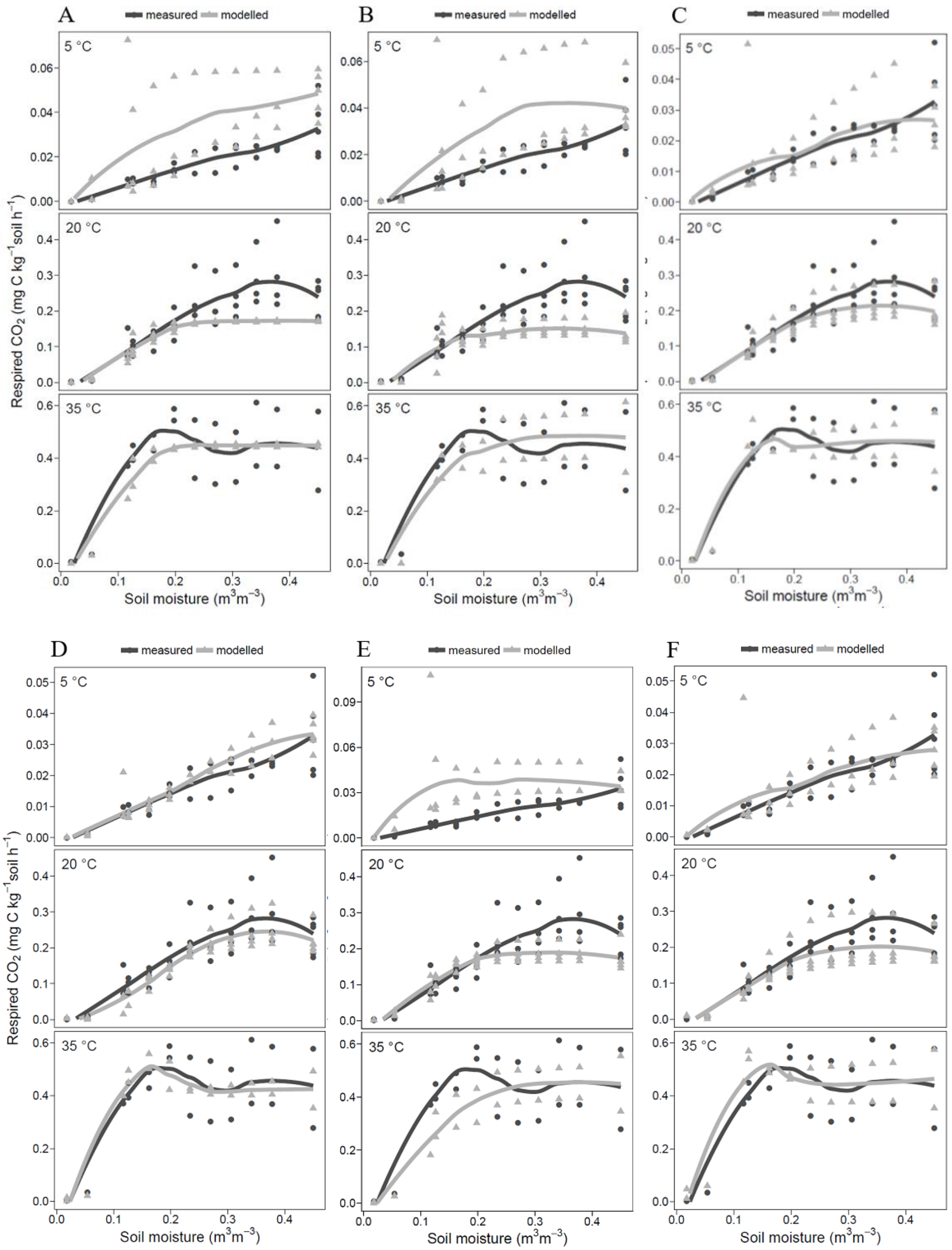

Figure S1: The relationship between respiration rates and soil moisture content shown for observations and diffusion based models with different reaction kinetics. Each plot compares the measurements with a different model. A: 11-dif, B: 22-dif, C: M1-dif, D: M2-dif, E: MM-dif, and F: Mr2-dif. The average relationship is depicted with smooth loess fits.

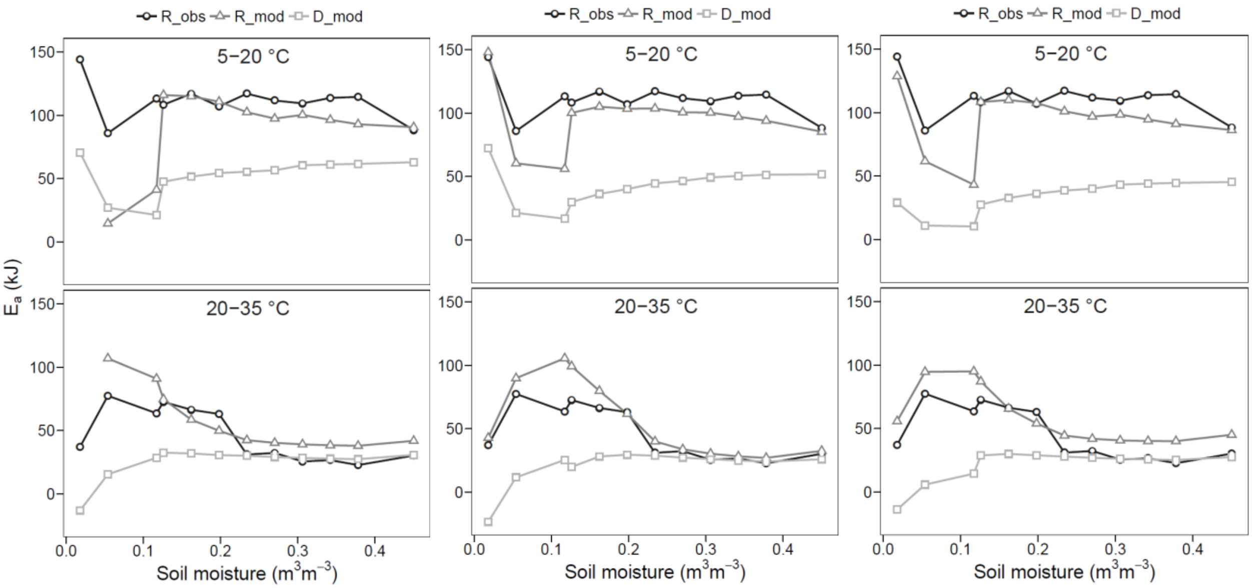

Figure S2: The relationship between apparent temperature sensitivities and soil moisture content shown for observations and M1-dif (left), M2-dif (middle) and M_r2-dif (right).

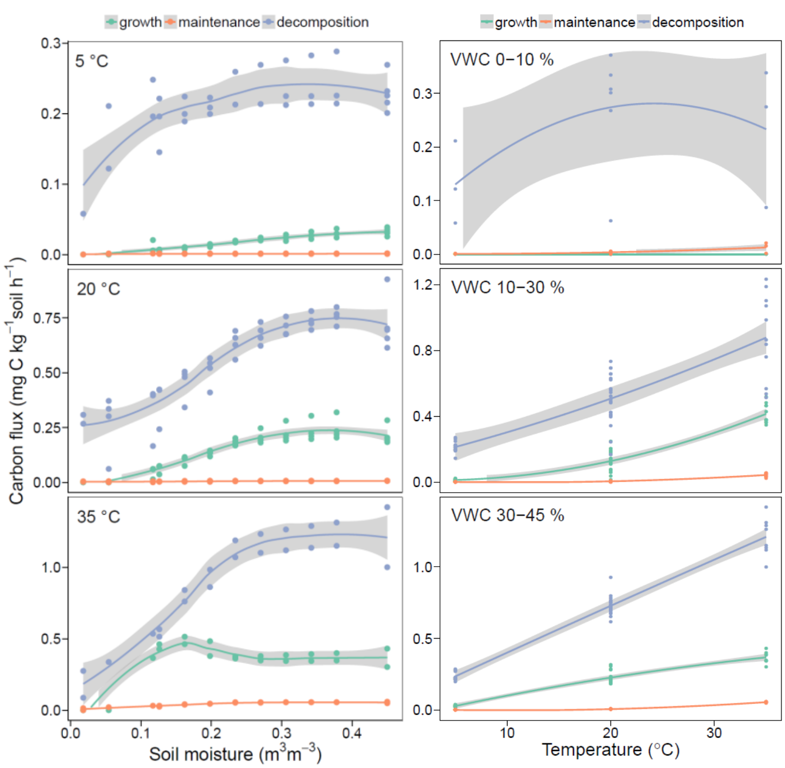

Figure S3: Modelled growth respiration, maintenance respiration and decomposition against soil moisture (left plot) and soil temperature (right plot) using model M2-dif.

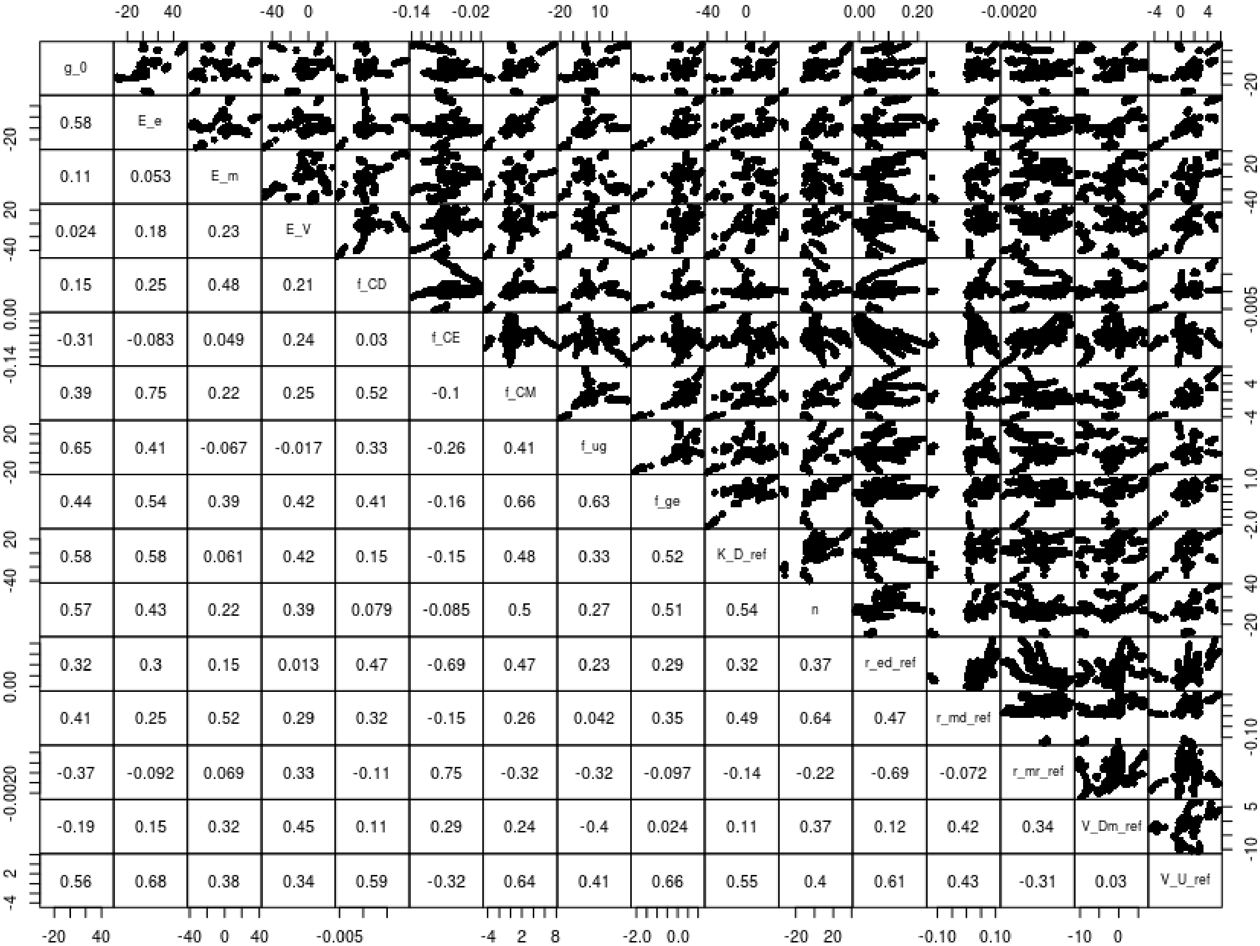

Figure S4: Correlations between sensitivity functions of model parameters (from R function sensFun, package FME). Parameters resulting in 0 sensitivity (*n*, θ_{th}) are excluded.

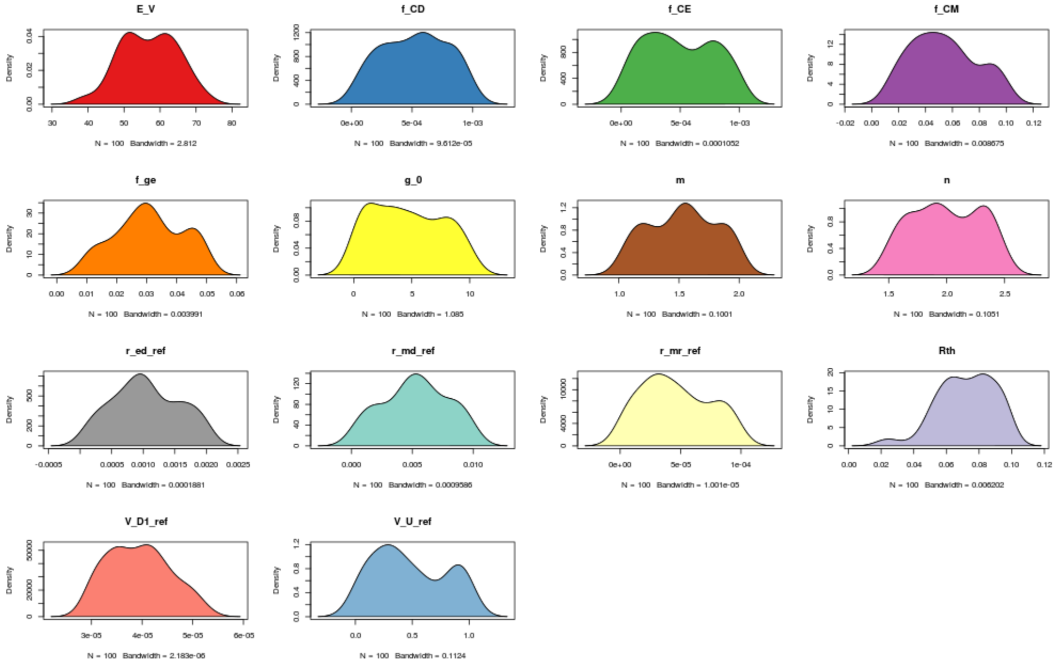

Figure S5: Kernel density estimations for model 11-dif. Estimations are made with the 100 parameter sets resulting in the lowest model cost from 30000 (Latin Hypercube).

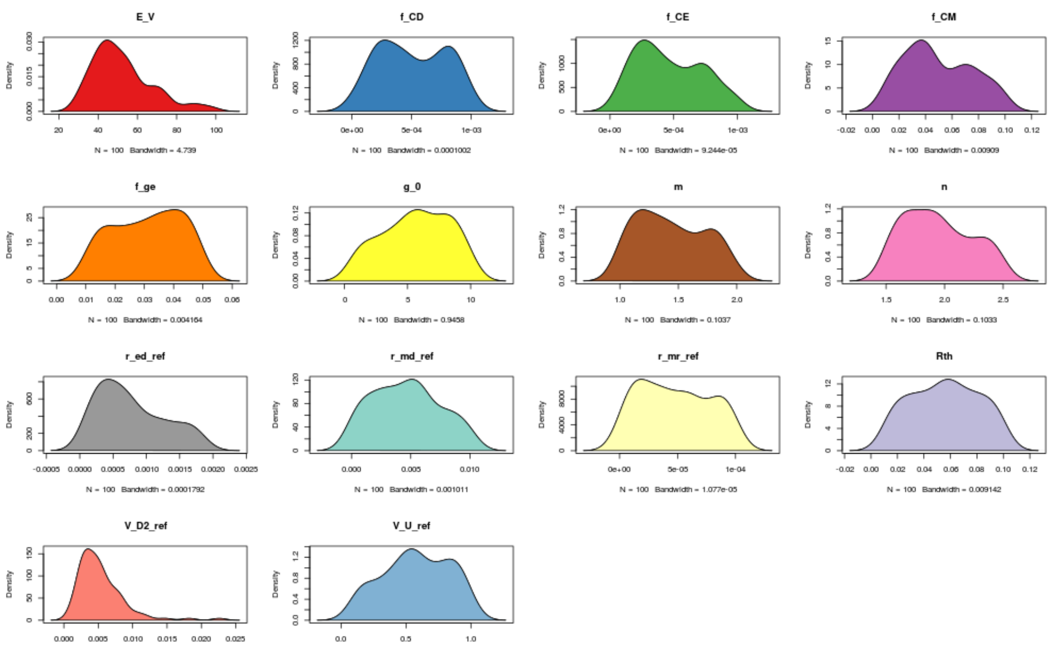

Figure S6: Kernel density estimations for model 22-dif. Estimations are made with the 100 parameter sets resulting in the lowest model cost from 30000 (Latin Hypercube).

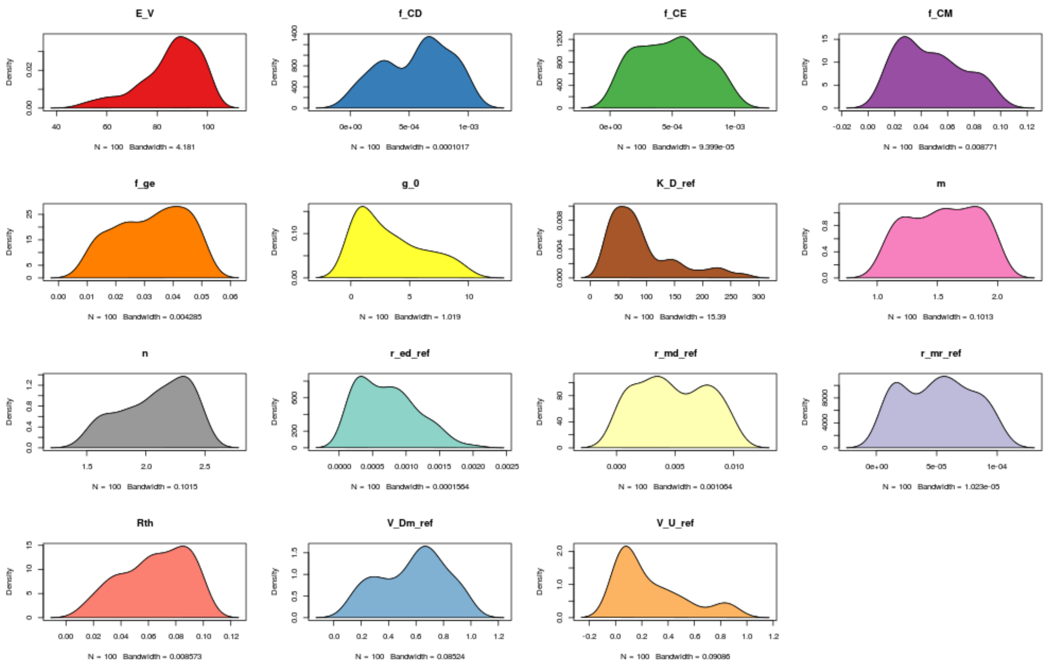

Figure S7: Kernel density estimations for model M1-dif. Estimations are made with the 100 parameter sets resulting in the lowest model cost from 30000 (Latin Hypercube).

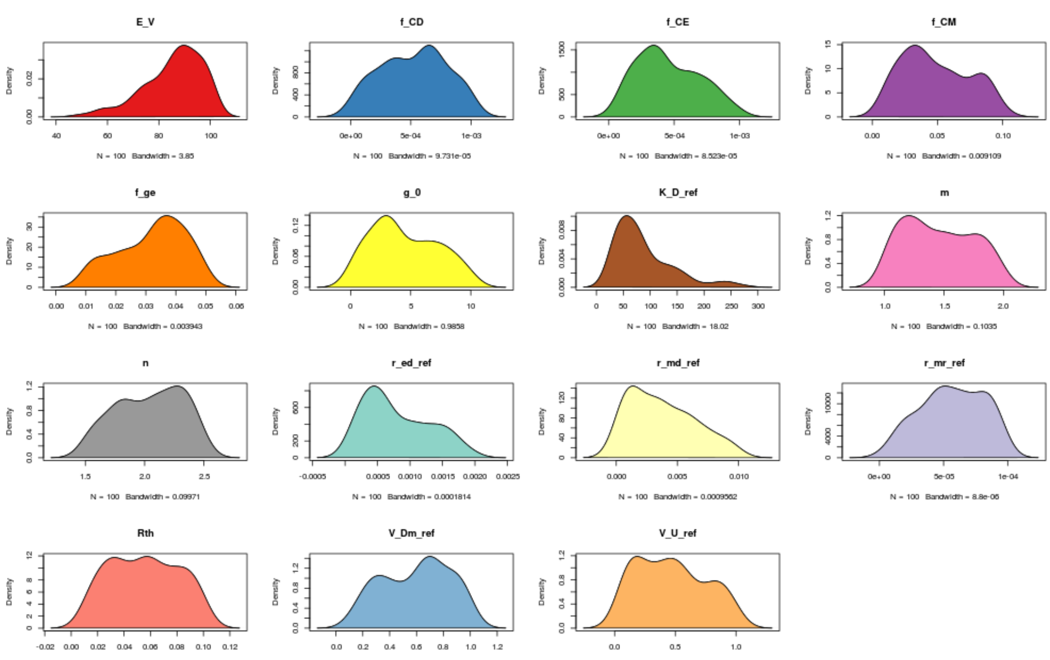

Figure S8: Kernel density estimations for model M2-dif. Estimations are made with the 100 parameter sets resulting in the lowest model cost from 30000 (Latin Hypercube).

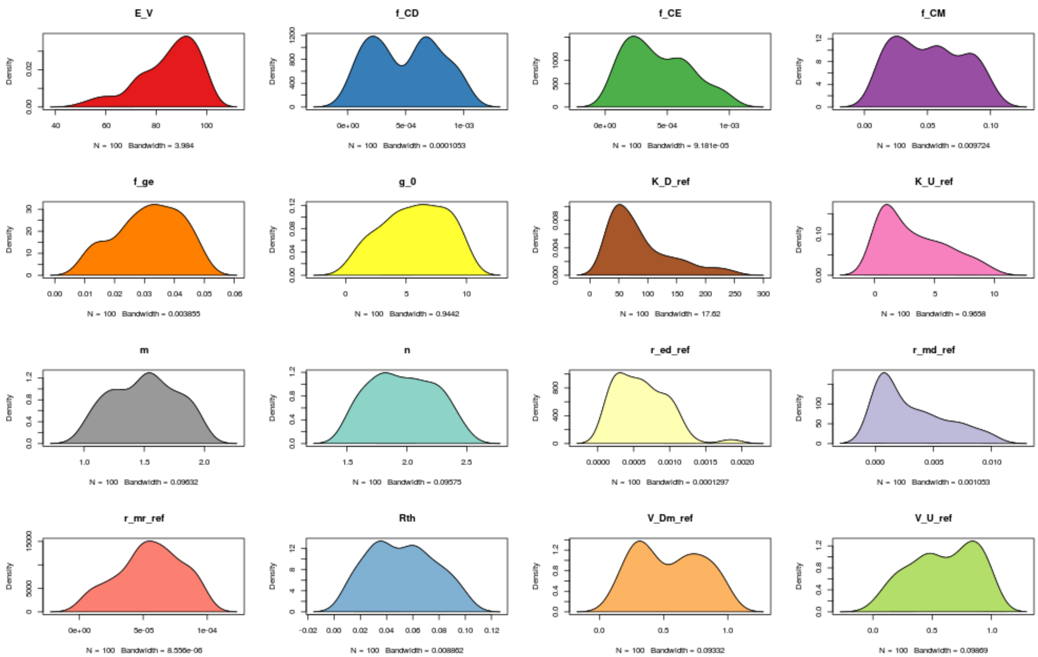

Figure S9: Kernel density estimations for model MM-dif. Estimations are made with the 100 parameter sets resulting in the lowest model cost from 30000 (Latin Hypercube).

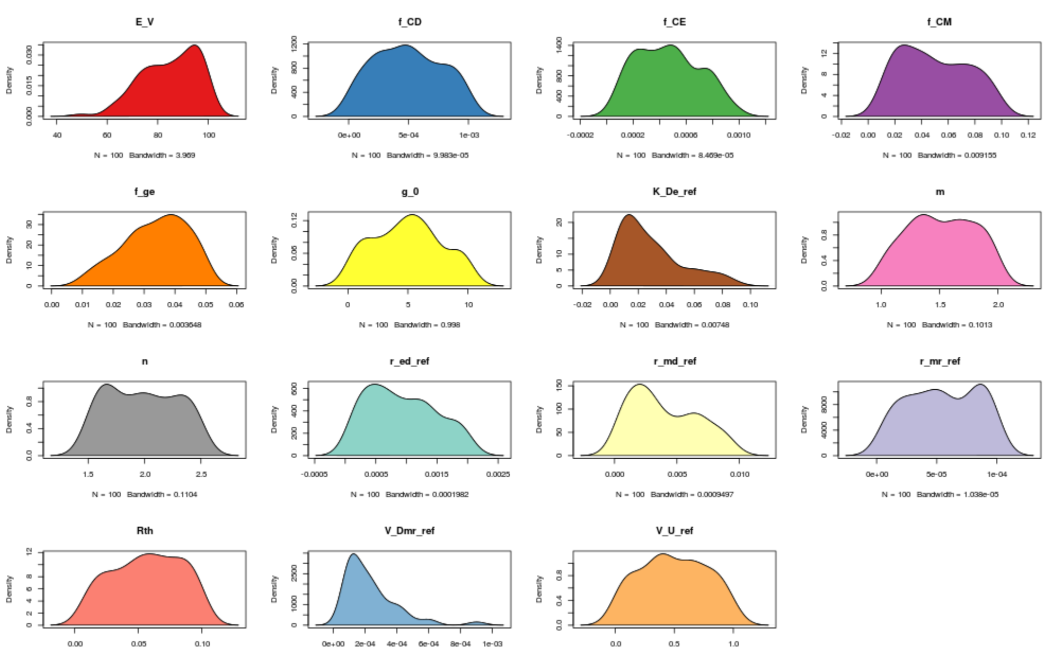

Figure S10: Kernel density estimations for model M_r2-dif. Estimations are made with the 100 parameter sets resulting in the lowest model cost from 30000 (Latin Hypercube).

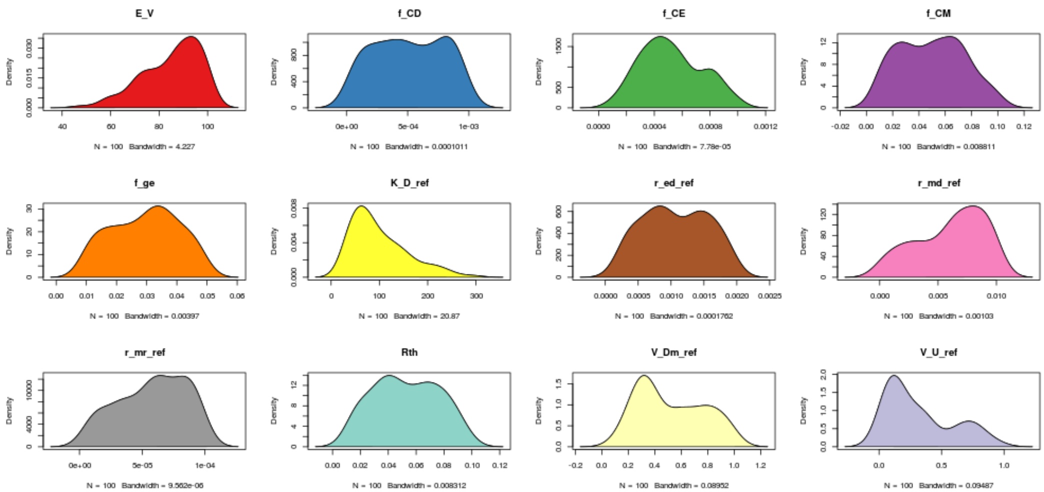

Figure S11: Kernel density estimations for model M2-psi. Estimations are made with the 100 parameter sets resulting in the lowest model cost from 30000 (Latin Hypercube).

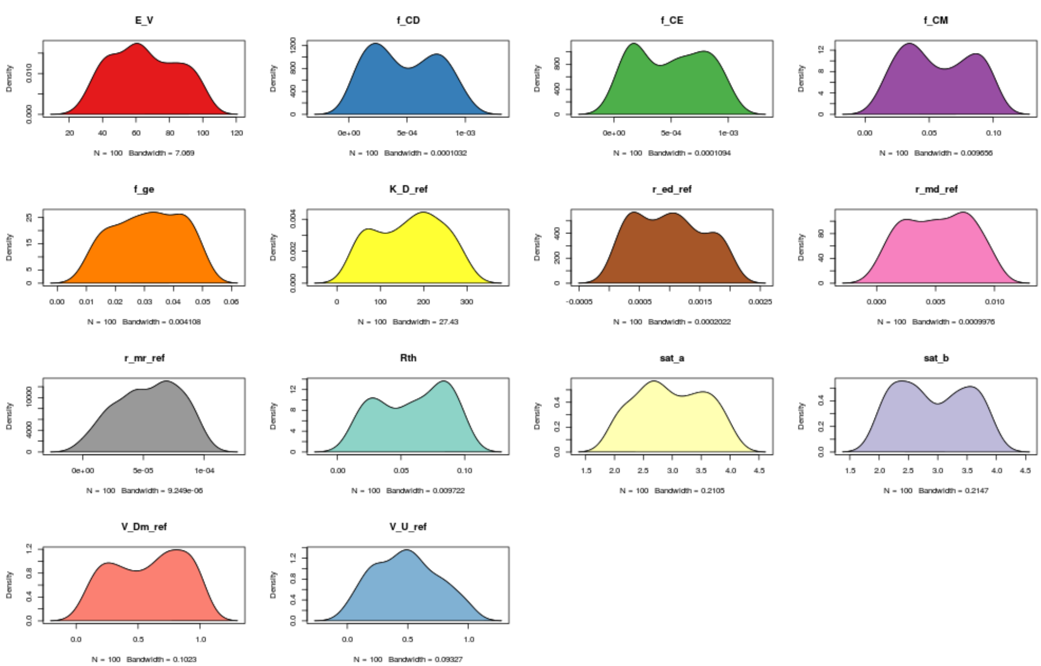

Figure S12: Kernel density estimations for model M2-sat. Estimations are made with the 100 parameter sets resulting in the lowest model cost from 30000 (Latin Hypercube).

Supplementary tables

Table S1: Calibrated model parameters with lower and upper bounds.

Symbol	Description	Units	Lower	Upper	References
E_V	Activation energy for VD_ref, VU_ref, rmr_ref, KD	kJ	30	100	(Price and Sowers, 2004; Tang and Riley, 2014; Wang et al., 2013)
f_D	Initial CD fraction of SOC	kg kg^{-1}	1.00E-05	0.001	-
f_E	Initial CEM, CED fraction of SOC	kg kg^{-1}	1.00E-05	0.001	-
f_M	Initial CM fraction of SOC	kg kg^{-1}	0.01	0.1	-
f_{ge}	Fraction of growth going to CEM	kg kg^{-1}	0.01	0.05	(Schimel and Weintraub, 2003)
g_0	Conductance for diffusion	h-1	0.1	10	(Hu and Wang, 2003; Jones et al., 2005; Manzoni et al., 2016; Vetter et al., 1998)
K_{D_ref}	Michaelis-Menten constant of decomposition Eq. (8)	kg C m^{-3}	30	300	-
K_{De_ref}	Michaelis-Menten constant of decomposition Eq. (9)	kg C m^{-3}	0.001	0.1	-
K_{U_ref}	Michaelis-Menten constant of uptake Eq. (8)	kg C m^{-3}	0.01	10	-
m	Exponent in Eq. (11)	-	1	2	(Hamamoto et al., 2010)
n	Exponent in Eq. (11)	-	1.5	2.5	(Hamamoto et al., 2010)
r_{ed_ref}	Reference rate of CEM, CED decay	h-1	0.0001	0.002	(Li et al., 2014)
r_{md_ref}	Reference rate of CM decay	h-1	0.0001	0.01	(Li et al., 2014)
r_{mr_ref}	Reference rate of maintenance respiration	h-1	1.00E-06	0.0001	(Price and Sowers, 2004)
θ_{th}	Moisture threshold for diffusion	m^3 m^{-3}	0.01	0.1	(Manzoni and Katul, 2014)
a	Moisture function coefficient Eq. (21)	-	2	4	(Moyano et al., 2013)
b	Moisture function coefficient Eq. (21)	-	2	4	(Moyano et al., 2013)
V_{D1_ref}	Reference rate of decomposition Eq. (6)	h-1	1.00E-05	0.001	(Li et al., 2014)
V_{D2_ref}	Reference rate of decomposition Eq. (7)	h-1	0.001	0.1	(Li et al., 2014)
V_{Dm_ref}	Reference rate of decomposition Eq. (8)	h-1	0.1	1	(Li et al., 2014)
V_{Dmr_ref}	Reference rate of decomposition Eq. (9)	h-1	1.00E-05	0.001	(Li et al., 2014)
V_{U_ref}	Reference rate of carbon uptake	h-1	0.01	1	(Li et al., 2014)

Table S2: Fixed model parameters.

Symbol	Description	References	Value	Units
E_e	Activation energy for r_{ed_ref}	(Grisi et al., 1998; Salazar-Villegas et al., 2016)	10	kJ
E_m	Activation energy for r_{md_ref}	(Grisi et al., 1998; Salazar-Villegas et al., 2016)	10	kJ
f_{ug}	Fraction of uptake to growth (i.e. CUE)	(Hagerty et al., 2014)	0.7	kg kg^{-1}
pd	Particle density	-	2700	kg m^{-3}
Ψ_{opt}	Optimal water potential Eq. (22)	-	33	kPa
Ψ_{th}	Threshold water potential Eq. (22)	-	15000	kPa
R	R gas constant	-	0.0083	-
T_{ref}	Reference temperature Eq. (20)	-	290	°K
sand	Soil sand fraction	-	0.28	kg kg^{-1}
silt	Soil silt fraction	-	0.57	kg kg^{-1}
clay	Soil clay fraction	-	0.15	kg kg^{-1}
ps	Soil pore space	-	0.45	m^3 m^{-3}
toc	Soil total organic carbon	-	0.012	kg
z	Soil depth	-	1	m
Ψ_{sat}	Saturation water potential	-	0.46	kPa

Table S3: Calibrated model parameters showing optimal values found for each model version. A missing value means the parameter was not part of the model.

Par	11-dif	22-dif	M1-dif	M2-dif	MM-dif	M2-psi	M2-sat	Mr2-dif
E_V	49	39	99	94	98	68	94	94
f_D	0.00014	2.50E-05	4.00E-05	9.10E-05	5.10E-05	0.00096	0.00018	0.001
f_E	9.20E-05	0.00021	0.00071	0.00068	0.00041	0.00057	0.00066	0.00042
f_M	0.092	0.012	0.085	0.08	0.012	0.015	0.065	0.042
f_{ge}	0.048	0.018	0.041	0.034	0.018	0.031	0.031	0.033
g_0	1.1	9	5.6	0.98	8.3	-	-	0.61
K_{D_ref}	-	-	53	62	31	100	180	-
K_{De_ref}	-	-	-	-	-	-	-	0.063
K_{U_ref}	-	-	-	-	1.1	-	-	-
m	1.9	1.1	1.3	1.1	1.7	-	-	1
n	2.4	2.3	2.3	2.3	2.5	-	-	2.2
r_{ed_ref}	0.0018	0.00056	0.00038	0.00056	0.00017	0.0016	0.00064	0.00025
r_{md_ref}	0.0087	0.0096	0.0036	0.00099	0.0016	0.0093	0.008	0.00059
r_{mr_ref}	5.50E-06	9.70E-05	8.90E-05	1.50E-05	9.80E-05	9.00E-05	8.80E-05	4.80E-05
θ_{th}	0.029	0.055	0.049	0.063	0.011	-	-	0.06
a	-	-	-	-	-	-	3.1	-
b	-	-	-	-	-	-	2.1	-
V_{D1_ref}	4.80E-05	-	-	-	-	-	-	-
V_{D2_ref}	-	0.0082	-	-	-	-	-	-
V_{Dm_ref}	-	-	0.23	0.37	0.22	0.65	0.57	-
V_{Dmr_ref}	-	-	-	-	-	-	-	0.00028
V_{U_ref}	0.082	0.75	0.018	0.11	0.19	0.11	0.15	0.18

References

Grisi, B., Grace, C., Brookes, P. C., Benedetti, A. and Dell'abate, M. T.: Temperature effects on organic matter and microbial biomass dynamics in temperate and tropical soils, Soil Biol. Biochem., 30(10–11), 1309–1315, doi:10.1016/S0038-0717(98)00016-9, 1998.

Hagerty, S. B., van Groenigen, K. J., Allison, S. D., Hungate, B. A., Schwartz, E., Koch, G. W., Kolka, R. K. and Dijkstra, P.: Accelerated microbial turnover but constant growth efficiency with warming in soil, Nat. Clim. Change, 4(10), 903–906, doi:10.1038/nclimate2361, 2014.

Hamamoto, S., Moldrup, P., Kawamoto, K. and Komatsu, T.: Excluded-volume expansion of Archie's law for gas and solute diffusivities and electrical and thermal conductivities in variably saturated porous media, Water Resour. Res., 46(6), doi:10.1029/2009WR008424, 2010.

Hu, Q. and Wang, J.: Aqueous-phase diffusion in unsaturated geologic media: A review, Crit. Rev. Environ. Sci. Technol., 33(3), 275–297, 2003.

Jones, D. L., Healey, J. R., Willett, V. B., Farrar, J. F. and Hodge, A.: Dissolved organic nitrogen uptake by plants—an important N uptake pathway?, Soil Biol. Biochem., 37(3), 413–423, doi:10.1016/j.soilbio.2004.08.008, 2005.

Li, J., Wang, G., Allison, S. D., Mayes, M. A. and Luo, Y.: Soil carbon sensitivity to temperature and carbon use efficiency compared across microbial-ecosystem models of varying complexity, Biogeochemistry, 119(1–3), 67–84, doi:10.1007/s10533-013-9948-8, 2014.

Manzoni, S. and Katul, G.: Invariant soil water potential at zero microbial respiration explained by hydrological discontinuity in dry soils, Geophys. Res. Lett., 41(20), 7151–7158, doi:10.1002/2014GL061467, 2014.

Manzoni, S., Moyano, F., Kätterer, T. and Schimel, J.: Modeling coupled enzymatic and solute transport controls on decomposition in drying soils, Soil Biol. Biochem., 95, 275–287, doi:10.1016/j.soilbio.2016.01.006, 2016.

Moyano, F. E., Manzoni, S. and Chenu, C.: Responses of soil heterotrophic respiration to moisture availability: An exploration of processes and models, Soil Biol. Biochem., 59, 72–85, doi:10.1016/j.soilbio.2013.01.002, 2013.

Price, P. B. and Sowers, T.: Temperature dependence of metabolic rates for microbial growth, maintenance, and survival, Proc. Natl. Acad. Sci. U. S. A., 101(13), 4631–4636, 2004.

Salazar-Villegas, A., Blagodatskaya, E. and Dukes, J. S.: Changes in the Size of the Active Microbial Pool Explain Short-Term Soil Respiratory Responses to Temperature and Moisture, Front. Microbiol., 7, doi:10.3389/fmicb.2016.00524, 2016.

Schimel, J. P. and Weintraub, M. N.: The implications of exoenzyme activity on microbial carbon and nitrogen limitation in soil: a theoretical model, Soil Biol. Biochem., 35(4), 549–563, 2003.

Tang, J. and Riley, W. J.: Weaker soil carbon–climate feedbacks resulting from microbial and abiotic interactions, Nat. Clim. Change, 5(1), 56–60, doi:10.1038/nclimate2438, 2014.

Vetter, Y. A., Deming, J. W., Jumars, P. A. and Krieger-Brockett, B. B.: A Predictive Model of Bacterial Foraging by Means of Freely Released Extracellular Enzymes, Microb. Ecol., 36(1), 75–92, doi:10.1007/s002489900095, 1998.

Wang, G., Post, W. M. and Mayes, M. A.: Development of microbial-enzyme-mediated decomposition model parameters through steady-state and dynamic analyses, Ecol. Appl., 23(1), 255–272, 2013.